euronoise

Green's function model for a Rijke tube with a distributed heat source

Maria Heckl

Keele University, Staffordshire, ST5 5BG Newcastle-under-Lyme, UK
m.a.heckl@keele.ac.uk

A Rijke tube is an open-ended tube with a compact heat source (flame or hot gauze) inside. The heat source is commonly modelled by the "nτ law", which assumes a point source releasing heat at a rate that is proportional to the velocity (delayed by a time lag τ) at the heat source. The present paper aims to extend this model to include distributed heat sources. A distributed source is simulated by a row of point sources with individual heat release rates and time lags. The acoustic processes in the tube will be modelled by Lighthill's acoustic analogy equation, combined with a Green's function approach. The occurrence of thermo-acoustic instabilities will be predicted for different properties of the heat source. Geometrical complications in the tube, such as a blockage and a jump in cross-section, as well as a jump in mean temperature, will be taken into account.

1 Introduction

1.1 Rijke tube configuration

We consider a Rijke tube with axisymmetric geometry; a cross-section between the tube axis and the tube wall is shown in Figure 1. The ends are open with pressure nodes just outside the tube at $x = \ell_1$ and $x = \ell_2$ (Rayleigh end correction). There is a blockage, a change of cross-sectional area from $\mathcal{A}_1$ to $\mathcal{A}_2$ and a jump in mean temperature from $\overline{T}_1$ to $\overline{T}_2$. The speed of sound jumps from c_1 to c_2 due to the temperature jump. The blockage, which is assumed to be compact, is modelled by an incompressible "airplug" of effective length L_{eff} oscillating parallel to the x-axis. L_{eff} depends on the geometry of the flame holder and has to be calculated numerically (see [1]). In the region around the blockage, the acoustic field is three-dimensional, but in the upstream region between $x = 0$ and X_1, as well as in the downstream region between $x = X_2$ and L, the field is one-dimensional.

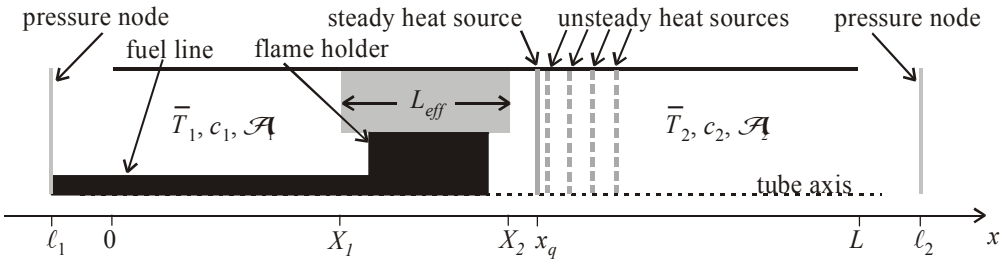

Figure 1 Rijke tube with multiple heat sources

The jump in mean temperature is caused by a steady heat source (marked by a solid grey line in Figure 1), which is situated near the downstream edge of the flame holder. The unsteady component of the heat source is represented by a distribution of point sources, shown in Figure 1 by broken grey lines.

1.2 The Green function

An important element of our theoretical model is the exact acoustic Green function $G(\mathbf{x}, \mathbf{x}', t, t')$. This is the velocity potential in the tube at position $\mathbf{x}$ and time t, created by an impulsive point source at position $\mathbf{x}'$ and time t'. The exact Green function is the solution of

$$\frac{1}{c^2}\frac{\partial^2 G}{\partial t^2} - \nabla^2 G = \delta(\mathbf{x} - \mathbf{x}')\delta(t - t'), \tag{1}$$

inside the tube (c is the speed of sound, taking values c_1 and c_2 in the upstream and downstream region, respectively) and satisfies the following boundary conditions: It is zero at $x = \ell_1$ and $x = \ell_2$ (this neglects losses from the ends), and it has a normal derivative equal to zero on all internal surfaces and on the tube axis. It also satisfies the conditions of reciprocity and causality. For the case where x' is in one of the one-dimensional regions, Green's function has the form

$$G(x, x', t - t') = \sum_{n=1}^{\infty} g_n(x, x')\,\mathrm{H}(t - t')\sin\omega_n(t - t'). \tag{2}$$

H is the Heaviside function, ω_n are the eigenfrequencies of the Rijke tube (with steady heating) and g_n are the modal amplitudes. Green's function is an impulse response: it is zero before the impulse (at $t = t'$) and consists of a superposition of eigenmodes (numbered by the index n) thereafter. Analytical expressions for ω_n and $g_n(x, x')$ have been derived in [1].

1.3 The heat source

The heat source is decomposed into several components, all of which are point sources. A steady component situated at x_q releases heat at a constant rate and only serves to increase the mean temperature. An array of unsteady heat sources is situated at discrete points x_m, $m = 1, 2, 3, \ldots M$; each of these sources releases heat to the air (per unit mass of air). The combined heat release rate from these unsteady sources is

$$q'(x,t) = \sum_{m=1}^{M} q_m(t)\delta(x - x_m)\,. \tag{3}$$

The heat release rate generally depends on aerodynamic fluctuations in the tube; this dependence is called the "heat release characteristic". We assume a dependence of the form

$$q_m(t) = q_m(\,u(x_m, t-\tau_m))\,, \tag{4}$$

i.e. the heat release rate from source m is a function of the acoustic velocity u at that source, delayed by a time lag τ_m.

2 Governing equation

The velocity potential ϕ in the Rijke tube is governed by the nonhomogeneous wave equation (see [2] p. 508; γ is the specific heat ratio),

$$\frac{1}{c^2}\frac{\partial^2\phi}{\partial t^2} - \frac{\partial^2\phi}{\partial x^2} = -\frac{\gamma-1}{c^2}q'(x,t)\,. \tag{5}$$

We will derive an integral equation from (5) and (1) by performing the following steps: Equation (5) and the one-dimensional form of (1) are written in terms of the source variables x' and t'; (1) is multiplied by $\phi(x',t')$, (5) by $G(x,x',t-t')$, and the resulting equations are subtracted. This gives

$$\phi(x',t')\delta(x-x')\delta(t-t') + \frac{\gamma-1}{c^2}Gq'(x',t') = \frac{1}{c^2}\left(\phi\frac{\partial^2 G}{\partial t'^2} - G\frac{\partial^2\phi}{\partial t'^2}\right) - \left(\phi\frac{\partial^2 G}{\partial x'^2} - G\frac{\partial^2\phi}{\partial x'^2}\right). \tag{6}$$

This equation is integrated with respect to x' (from ℓ_1 to ℓ_2) and t' (from 0 to t). For a heat release rate of the form (3), the result can be simplified (using the boundary conditions at the tube ends) to give

$$\phi(x,t) = -\frac{\gamma-1}{c^2}\sum_{m=1}^{M}\int_{t'=0}^{t} G(x,x_m,t-t')\,q_m(t')\,\mathrm{d}t' + \int_{x'=\ell_1}^{\ell_2}\frac{1}{c^2}\left[\phi\frac{\partial G}{\partial t'} - G\frac{\partial\phi}{\partial t'}\right]_{t'=0}^{t}\mathrm{d}x'\,. \tag{7}$$

We assume the following initial conditions:

$$\phi(x',t')\big|_{t'=0} = 0 \quad\text{and}\quad \left.\frac{\partial\phi(x',t')}{\partial t'}\right|_{t'=0} = 0 \quad\text{for all } x'\in(\ell_1,\ell_2)\,, \tag{8}$$

i.e. the velocity and acceleration are zero throughout the tube at the time $t'=0$. Combined with causality of the Green function ($G=0$ and $\frac{\partial G}{\partial t'}=0$ for $t'\le t$), equation (7) then simplifies, due to the second integral on the right hand side becoming zero.

The remainder of (7) can be turned into an equation for the velocity by differentiating with respect to x. Evaluation at $x = x_1, x_2, \ldots x_M$ leads to a set of integral equations giving the velocity at the heat sources in terms of the heat release rate,

$$u_j(t) = -\frac{\gamma-1}{c^2}\sum_{m=1}^{M}\int_{t'=0}^{t}\left.\frac{\partial G(x,x',t-t')}{\partial x}\right|_{\substack{x=x_j\\x'=x_m}} q_m(t')\,\mathrm{d}t'\,, \qquad j = 1, 2, \ldots M\,; \tag{9}$$

the abbreviation $u_j(t) = \left.\frac{\partial\phi(x,t)}{\partial x}\right|_{x=x_j}$ has been introduced for the velocity at the heat source j.

3 Numerical solution

The x-derivative of Green's function is calculated from (2) and inserted into (9). This gives (using complex notation)

$$u_j(t) = \frac{\gamma-1}{c^2}\,\mathrm{Im}\left[\sum_{n=1}^{\infty}\mathrm{e}^{-\mathrm{i}\omega_n t}\sum_{m=1}^{M}\left.\frac{\partial g_n(x,x')}{\partial x}\right|_{\substack{x=x_j\\x'=x_m}}\int_{t'=0}^{t}\mathrm{e}^{\mathrm{i}\omega_n t'}q_m(t')\,\mathrm{d}t'\right]. \tag{10}$$

The integral in (10), $I_{mn}(t) = \int_{t'=0}^{t}\mathrm{e}^{\mathrm{i}\omega_n t'}q_m(t')\,\mathrm{d}t'$, can be split into two parts, one over the interval $(0, t-\Delta t)$, and the other over an interval of width Δt, where Δt is a small time step,

$$I_{mn}(t) = \int_{t'=0}^{t-\Delta t}\mathrm{e}^{\mathrm{i}\omega_n t'}q_m(t')\,\mathrm{d}t' + \int_{t'=t-\Delta t}^{t}\mathrm{e}^{\mathrm{i}\omega_n t'}q_m(t')\,\mathrm{d}t'\,. \tag{11}$$

The first integral represents $I_{mn}(t-\Delta t)$. The second integral can be approximated: the time interval Δt is assumed to be very small, and therefore the heat release rate in this time interval is nearly constant and equal to $q_m(t-\Delta t)$. With these results,

(11) can be written as

$$I_{mn}(t) = I_{mn}(t-\Delta t) + q_m(t-\Delta t)\frac{\mathrm{e}^{\mathrm{i}\omega_n t}}{\mathrm{i}\omega_n}\left(1-\mathrm{e}^{-\mathrm{i}\omega_n \Delta t}\right), \tag{12}$$

and this leads with equation (10) to

$$u_j(t) = \frac{\gamma-1}{c^2}\,\mathrm{Im}\left[\sum_{n=1}^{\infty}\mathrm{e}^{-\mathrm{i}\omega_n t}\sum_{m=1}^{M}\left.\frac{\partial g_n(x,x')}{\partial x}\right|_{\substack{x=x_j \\ x'=x_m}} I_{mn}(t)\right]. \tag{13}$$

Equations (12) and (13) comprise an iteration procedure for the time history of the velocity $u_j(t)$, and also for that of the heat release rate $q_m(t)$ (see equation (4)). They are solved by stepping forward in time with steps Δt. The starting point of the iteration is provided by the initial condition $u_m(t-\tau_1)\big|_{t=0} = u_0$ (this precedes the initial conditions specified in (8)).

4 Numerical results and discussion

4.1 Rijke tube configuration

The iteration described by equations (12) and (13) was performed numerically for a tube with the following properties:

$L = 1$ m (tube length), $\ell_1 = -0.014$ m, $\ell_2 = 1.014$ m, $\frac{\mathcal{A}_2}{\mathcal{A}_1} = 1.128$, $L_{eff} = 0.093$ m,

$\bar{T}_1 = 288$ K (room temperature), $\bar{T}_2 = 488$ K, $c_1 = 342$ m s^{-1}, $c_2 = 446$ m s^{-1}.

The steady heat source was located at $x_q = 0.3L$. The eigenfrequencies of the first two modes are $\omega_1 = 1235\ \mathrm{s}^{-1}$ and $\omega_2 = 2722\ \mathrm{s}^{-1}$. A distribution of 4 sources was considered. These were situated at the positions x_1, x_2, x_3, x_4, and had a linear heat release characteristic,

$$q_m(t) = \beta\, u(x_m, t-\tau_m), \tag{14}$$

with time lags $\tau_1, \tau_2, \tau_3, \tau_4$. β, which is a measure for the strength of the heat source, had the constant value $\beta = 0.25 \cdot 10^6$ ms^{-3}. The time histories for the velocities and heat release rates were calculated as described in section 3, and from the resulting graphs, the stability behaviour of modes 1 and 2 was determined.

4.2 Results for a single point source

In order to be able to understand the results for a distributed source, we first consider a tube with a single point source and note how its stability behaviour depends on the source position and on the time lag. The calculations for the single-source case were done with the frequency-domain approach described in [3]. The results are shown in figures 2 and 3, giving the growth rate of mode 1 and mode 2. A positive growth rate indicates instability, a negative growth rate stability.

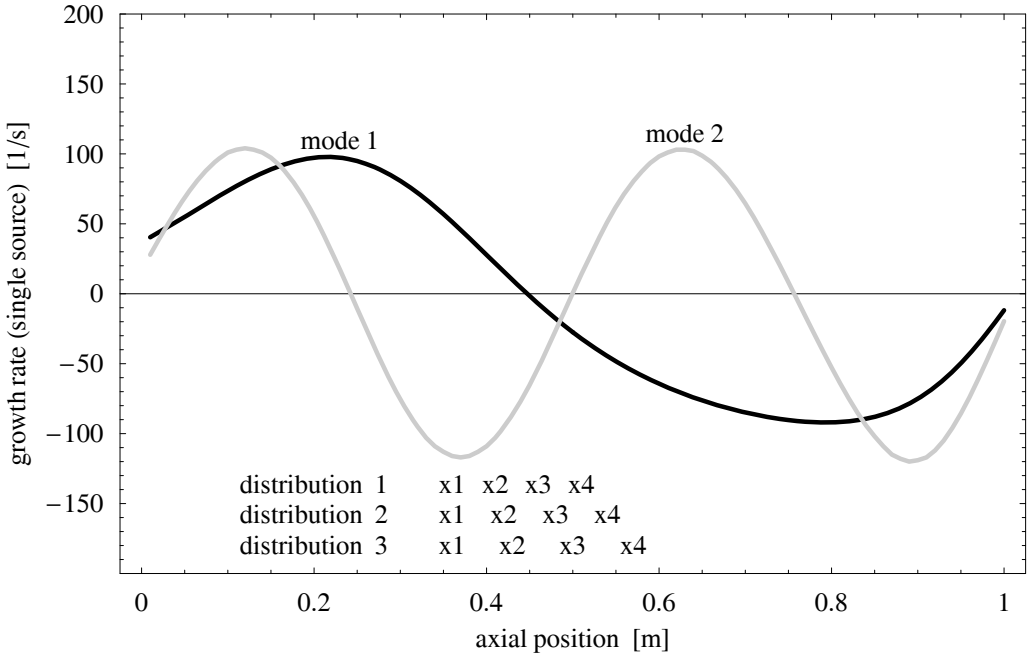

Figure 2 Stability behaviour of a single source: influence of the heat source position

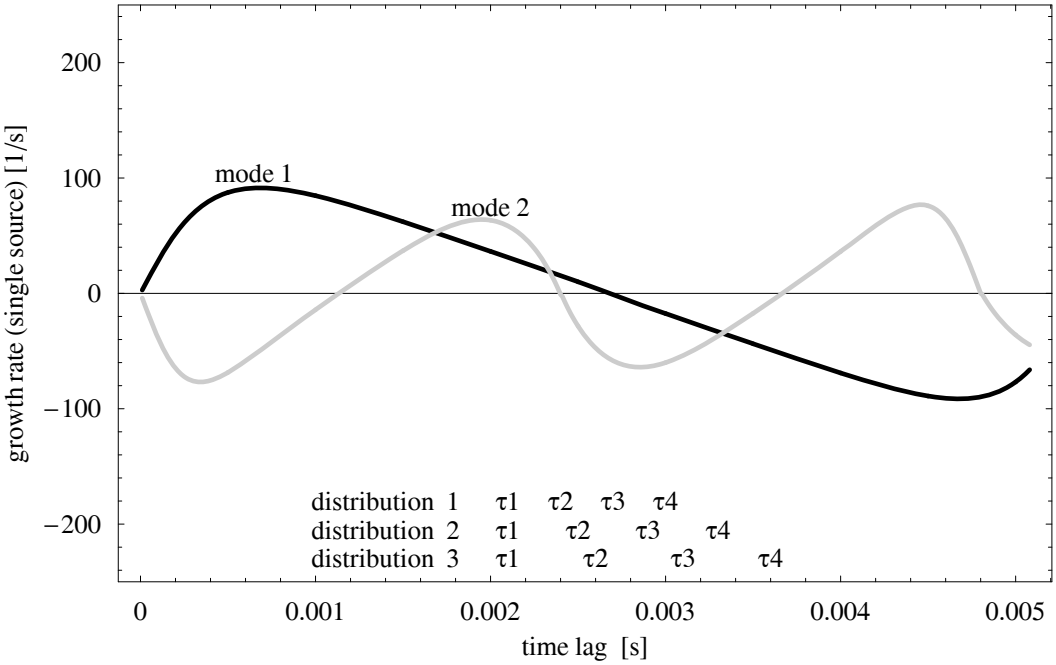

Figure 3 Stability behaviour of a single source: influence of the time lag

Figure 2 shows the dependence on the source position, covering the whole length of the tube. The time lag is constant, $\tau = 0.0004\,\mathrm{s}$, which is about 8% of the period of mode 1 (fundamental period). Mode 1 is unstable if the position is in the upstream half of the tube and stable in the downstream half; for mode 2 there are four regions of stability/instability, each spanning roughly a quarter of the tube length.

Figure 3 shows the dependence on the time lag and covers the whole of the fundamental period. The source is situated at $0.3L$, about ⅓ of the tube length from the upstream end. Mode 1 is unstable if the time lag is within the first half of the fundamental period and stable in the second half; for mode 2 there are (just over) four intervals of stability/instability, each spanning roughly a quarter of the fundamental period.

4.3 Influence of the heat source positions

Four unsteady heat sources, distributed in various patterns along the tube axis were considered, and the stability behaviour of modes 1 and 2 was examined. The time lag was kept constant, $\tau_m = 0.0004\,\mathrm{s}$. Mode 1 was always unstable if all four sources were in the upstream half of the tube, and always stable if they were in the downstream half. This is not surprising, given the behaviour of a single source, which was shown in figure 2. If the sources were distributed in the upstream *and* the downstream half, a sudden change in stability behaviour was found. The stability results for three such distributions are shown in table 1. The source positions are shown graphically (to scale) near the bottom of figure 2.

distribution	$x_1[m]$	$x_2[m]$	$x_3[m]$	$x_4[m]$	mode 1	mode 2
1	0.36	0.41	0.46	0.51	unstable	stable
2	0.36	0.42	0.48	0.54	marginally stable	stable
3	0.36	0.43	0.50	0.57	stable	stable

Table 1 Stability behaviour of modes 1 and 2 for three different source distributions

The sudden change occurs irrespective of the length of the region covered by the sources. It is due to the heat sources in the upstream half acting like a source of acoustic energy, while the ones in the downstream half act like sinks. The overall effect depends sensitively on the source distribution. When modelling combustion instabilities, it is often assumed that the heat source is small compared with the acoustic wavelength and can therefore be treated as a source concentrated at one point ("compact source"). The above results show that this approach can be too sweeping; care needs to be taken when the heat source is distributed along a stretch about half-way down the Rijke tube.

4.4 Influence of the time lags

Four sources, all at positions $x_m = 0.3L$, but with various time lags were considered, and the stability behaviour of modes 1 and 2 was examined. Mode 1 was always unstable if all four time lags were within the first half of the fundamental period and stable if they were in the second half. This is to be expected, given the behaviour of a single source, shown in figure 3. If the time lags were distributed in the first *and* the second half of the fundamental period, the stability behaviour depended critically on the distribution. This is shown for three such time-lag distributions in table 2. The time lags are indicated (to scale) near the bottom of figure 3.

distribution	$\tau_1[s]$	$\tau_2[s]$	$\tau_3[s]$	$\tau_4[s]$	mode 1	mode 2
1	0.0021	0.0024	0.0027	0.0030	unstable	stable
2	0.0021	0.0025	0.0029	0.0033	marginally stable	stable
3	0.0021	0.0026	0.0031	0.0036	stable	stable

Table 2 Stability behaviour of modes 1 and 2 for three different time-lag distributions

These results show that heat sources with different time lags can cancel one another as acoustic sources. This has also been observed by van Kampen [4], who used a transfer matrix method. Combustion instabilities are often modelled with a heat release characteristic that contains time lags to describe different travel times to different points along an extended flame; typically, such models are simplified by replacing the individual time lags with a single time lag, which is some average of the individual time lags. The above results show that this can work well, but that care needs to be taken, especially when the individual time lags are distributed around a value, which is near one half of the fundamental period.

5 Conclusions and outlook

A Green's function approach has been presented to model the behaviour of a Rijke tube with a distributed heat source. The heat source was discretised and represented by individual point sources at positions x_m. Each individual point source had its own linear heat release characteristic, described by an $n\tau$ law with individual time lags τ_m. Several different distributions of x_m and τ_m were simulated. The results confirmed that the distributed heat source can often be described by a single point source with a suitably chosen position and time lag. However, they also highlighted some cases where this approach can lead to errors in the stability predictions.

The approach can be extended to include nonlinear heat release characteristics. It can also be used for Rijke tubes with multiple sources anywhere in the tube.

References

[1] Maria A. Heckl and M.S. Howe, "Stability analysis of the Rijke tube with a Green's function approach". *Journal of Sound and Vibration* 305, 672-688 (2007)

[2] M.S. Howe, *Acoustics of fluid-structure interactions,* Cambridge University Press, 1998.

[3] Maria A. Heckl and M.S. Howe, "The Rijke tube: Green's function approach in the time and frequency domain", Proceedings of the 14th International Congress on Sound and Vibration, Cairns, Australia, 9-12 July 2007.

[4] J. van Kampen, "A one-dimensional approach to model thermoacoustic instabilities". Private communication, 21 November 2002.